Enhanced life-cycle supercapacitors by thermal treatment of mesophase-derived activated carbons

V. Ruiz, C. Blanco*, M. Granda and R. Santamaría

Instituto Nacional del Carbón, CSIC, Apdo. 73, 33080-Oviedo, Spain

Abstract.-

This paper studies the effect of thermal treatment on the long-term performance of carbon-based supercapacitors. Two active electrode materials were studied: a mesophase derived activated carbon (AC), rich in oxygen functionalities, and an activated carbon obtained from treating AC at 1000 °C (AC-1000), from which most of the functionalities had been removed. Up to 10,000 cycles were performed in aqueous acidic media at different voltage windows (0.6 and 1 V). Both materials showed an excellent life cycle, although the thermally treated carbon showed a significantly better behavior. The initial capacitance of AC-1000 was reduced by only ~5 % after 10,000 cycles, independently of the operating voltage, demonstrating that the thermal treatment of AC produces a very stable electrode material at both ranges of potential. The better performance of AC-1000 was attributed to the absence of functional groups and the higher degree of crystalline order that renders materials more stable. The use of these two materials in an asymmetric device resulted in a capacitor that merges both high stability and high capacitance values. The initial capacitance was reduced by only 4.5 % after 10,000 galvanostatic cycles and by 10 % after 20,000.

Key words: Activated carbon, electrochemical capacitor, double layer, pseudocapacitance, long-term cycling

*Corresponding author: clara@incar.csic.es; tlf: +34 985 11 90 90 fax.: + 34 985 29 76 62

1.- INTRODUCTION

Supercapacitors (SC's) are very attractive power storage devices because of their fast energy delivery [1]. These devices are suitable in many applications (e.g. telecommunications systems, maintenance-free traffic lights, uninterruptible power sources, UPS's, etc.), but it is in the field of transport where their properties are best suited as they can provide power peaks during acceleration and recover the energy lost from decelerating or braking. In addition, compared to other energy storage devices, supercapacitors have a much longer life cycle (> 100,000 cycles), this being one of their main characteristics.

Carbon materials have proved to be ideal candidates for use in SC's because of their high surface area, which displays different kinds of porosity and surface functionalities. These materials can be obtained in a wide variety of forms at relatively low cost. In general terms, the presence of heteroatoms in carbon materials, usually in the form of oxygen and nitrogen [2,3], is known to influence the involvement of pseudocapacitance due to faradaic charge transfer reactions [4,5] (e.g. quinone/hydroquinone redox couple, reversible electrosorption of hydrogen, etc.), wettability, point of zero charge, electrical conductivity and self-discharge characteristics, etc. [6]. Many authors have discussed the role of heteroatoms on the surface of carbon active materials on their electrochemical behavior [7-10]. Apart from the influence that surface functionalities have on specific capacitance values [7,8], they also play a role in degradation processes such as those that occur in electrodes, electrolyte [9] and auto-discharge reactions [10]. Generally, the presence of pseudocapacitance is related to a poor life cycle [11,12].

The type of electrolyte used to prepare the SC is also important, as it determines not only the operating voltage and ionic conductivity, but also the presence or absence of faradaic reactions [5]. Most of the commercially available supercapacitors use organic media [11] as, in this way, a high voltage window can be achieved (2-2.5 V) [13,14]. It is for this reason that non-aqueous electrolytes are preferred for high energy applications. Some ageing effects in organic-based supercapacitors have been attributed to the presence of surface functionalities, water or impurities in the active material [15], but in general pure charge separation occurs in organic media [5] and good cycling stability is typically reported [16].

Aqueous media (e.g. H_2SO_4, KOH) are restricted by their low electrochemical stability window (~ 1.23 V). However, they have the advantage of a high ionic conductivity, a characteristic which should contribute to the construction of high power density devices [5]. Moreover, the value of dielectric conductivity is higher and, therefore, the specific capacitance values are usually higher than in non-aqueous electrolytes [5]. Additionally, they have a low ionic size so accessibility restrictions are rarely reported. Although in this medium pseudocapacitative reactions are more likely to occur, with a consequent deterioration in cyclability, the incorporation of aqueous media in commercial systems would offer many advantages. Apart from those mentioned above, the assembly procedure would not require an inert atmosphere and the residues would be less toxic than in aprotic media. In theory, therefore, its commercialization should be safer, cheaper and more environmentally friendly [5]. However, until now few studies have been published on the causes of the deterioration of aqueous-based SC performance.

In a previous study [17] we evaluated the effect of the thermal treatment of a mesophase-derived activated carbon on its electrochemical performance. This treatment

led to a reduction in surface area and specific capacitance values (in part due to the elimination of functional groups and a reduction in its pseudocapacitative contribution), together with an improvement in electrical conductivity. In the present study the effect of thermal treatment on the long-term performance of the active materials was evaluated. Up to 10,000 cycles were performed in aqueous acidic media at different voltage windows (0.6 and 1 V). Cyclic voltammetry, impedance spectroscopy and galvanostatic cycling in two/three-electrode cells were employed in order to investigate and assess the phenomena that occur during long-term cycling.

The results obtained were used to build an asymmetric capacitor combining both activated carbons. Asymmetric systems have already been tested with conducting polymers and metal oxides [18,19], but systems that combine carbon materials with different properties are rarely found [20,21] and none of these have been tested in aqueous media.

2.- EXPERIMENTAL

2.1.- Active material and electrode preparation.-

The naphthalene derived mesophase pitch AR24 was chemically activated using potassium hydroxide in a proportion of 3:1 KOH to carbon at 700 ºC for 1 hour, under a nitrogen flow of 62 ml min^{-1} [22]. The resultant activated carbon was labeled AC. In order to study the effect of the removal of oxygenated functional groups on long-term cycling performance, AC was thermally treated at 1000 ºC for one hour at a heating rate of 2.5 ºC min^{-1} under a flow of nitrogen (62 mL min^{-1}). The resultant carbonized material was labelled AC-1000.

Coin-type electrodes were prepared using 10 wt. % of polyvinylidene fluoride (PVDF) as binder and 90 wt. % of active material (AC or AC-1000). These two components were mixed on a dry basis before they were pressed into electrodes. These electrodes were then dried overnight before any measurements were performed.

2.2.- Characterization of materials.-

Physical adsorption of nitrogen at 77 K was carried out in order to characterize the porous texture of the activated carbons and carbon-based electrodes. Isotherms were performed in an *ASAP 2020 Micromeritics* volumetric system using around 50 mg of sample for each measurement. The apparent specific surface area was determined from the N_2-adsorption isotherm using the BET equation. The total micropore volume (V_{N2}) was calculated by applying the Dubinin-Radushkevich (DR) equation to the N_2 isotherm [23]. The total pore volume was obtained from N_2 adsorption at P/P^0= 0.99 and the volume of mesopores was calculated by subtracting the total micropore volume (V_{N2}) from the total pore volume. The microporous surface area was obtained from the equation: S_{mic} (m^2 g^{-1}) = 2000V_{N2} (cm^3 g^{-1})/L_0 (nm) and the micropore volume, V_{N2}, was calculated by means of the DR equation.

The activated carbons were characterized by elemental analyses and the oxygen was determined directly using a LECO-TF-900 furnace coupled to a LECO-CHNS-932 microanalyzer. The surface oxygen functionality was studied by X-ray photoelectron spectroscopy (XPS) using a VG-Microtech Multilab 3000 spectrometer equipped with a hemispherical electron analyzer and a Mg K_(*hv* = 1253.6 eV) X-ray source.

The amount and type of oxygenated functionalities were determined by temperature-programmed decomposition (TPD) under an inert atmosphere (He). About

150 mg of sample was placed in a U-shaped quartz cell and heat treated to 1000 ºC at an increasing temperature of 10 ºC min^{-1}. The decomposition products (CO and CO_2) were identified by means of on-line mass spectrometer.

2.3.-Electrochemical measurements.-

Two-electrode capacitors were assembled in a Swagelok® cell using an aqueous solution of 1M sulfuric acid as electrolyte. A "T"-type cell was employed to prepare the capacitors. This configuration makes it possible to determine the potential at which the anode and cathode are operating, as the cell can be adapted to work either in a two- or three-electrode cell. In the case of the three-electrode cell, the reference electrode used was Hg/Hg_2SO_4 while a composite activated carbon/PVDF acted as the counter electrode. Asymmetric capacitors were built, using AC as active material in the negative electrode and AC-1000 in the positive one.

The electrochemical measurements were conducted in a *Biologic* multichannel potenciostat. Galvanostatic cycling at a current load of 500 mA g^{-1} was performed for the long-term cycling experiments at two different operating voltages: 0.6 and 1 V, up to 10,000 cycles. The capacitance of the system was obtained from the discharge branch of the galvanostatic cycles (avoiding the ohmic drop). Cyclic voltammetry experiments were carried out at 1 mV s^{-1}. Impedance spectroscopy analyses were conducted at 0 V. The frequencies used varied between 1 mHz-100 kHz at an amplitude of ±10 mV. These experiments were performed every 1,000 cycles in order to assess any changes experienced by the electrochemical cells.

3.- RESULTS AND DISCUSSION

3.1.-Textural and chemical characteristics of the activated carbons.-

The textural and chemical properties of the active materials used in the present study have been described elsewhere [17]. AC and AC-1000 are mainly microporous activated carbons with microporous surface areas of 1531 and 1318 $m^2 g^{-1}$, respectively. The apparent BET area is 2000 $m^2 g^{-1}$ for AC and 1600 $m^2 g^{-1}$ for AC-1000. This reduction in surface area has been attributed to the densification of the carbon materials when heated [24,25].

Regarding their chemical properties, AC has a significant amount of oxygenated functionalities, 3.5 wt. % as determined by elemental analysis and 9.0 wt. % as determined by XPS. The considerably higher values of XPS in comparison to those of the elemental analysis indicate that oxygen is mainly located in the surface of the carbons. These functionalities explains the acidic character of AC (pH= 2.8). By contrast AC-1000, which contains almost no functionalities (0.33 wt. % by elemental analysis and 2.5 wt. % by XPS) has neutral character (pH=7.5). The amount of CO_2 and CO evolved upon heating was calculated from the TPD profiles. CO_2 evolves at low temperatures due to the decomposition of carboxylic groups, lactones or anhydrides. CO evolution occurs at higher temperatures due to the decomposition of basic or neutral groups such as phenols, ethers and carbonyl groups [26]. In the case of the activated carbons in this study, CO evolved in larger amounts than CO_2: 1.223 versus 0.225 mmol g^{-1} for AC and 0.134 versus 0.080 for AC-1000. As expected, after treatment at 1000 ºC most of the oxygenated functional groups were eliminated.

3.2.-Electrochemical behavior

3.2.1.- Symmetric configuration

The dependence of the specific capacitance values of AC and AC-1000 on the number of cycles at two different operating voltages (0.6 and 1 V) is represented in Figure 1. In all cases, the efficiency of the capacitors remains close to 100 % during the long-term experiments, indicating that the reactions that occur in the cells do not affect their performance. Indeed, both materials demonstrate a good cycling performance, although some significant differences should be pointed out. As might be expected, when the voltage window is increased from 0.6 to 1 V, the stability of the AC cell deteriorates with cycling. However, AC-1000 maintains its excellent performance independently of the voltage window. For both materials the reduction in specific capacitance values is more pronounced during the first 4,000 cycles, after which they tend to stabilize.

The reduction in the specific capacitance values for AC was estimated as 12 % after 10,000 galvanostatic cycles performed at a low voltage window (0.6 V) and as 17 % in the case of 1 V, due to the higher involvement of irreversible reactions related to faradaic reactions (e.g. redox reactions of the oxygenated functional groups and/or irreversible oxidation of the carbonaceous structure). Despite these reductions, the specific capacitance values are still higher, even after 10,000 cycles, than those obtained at the lower potential window (200 *versus* 170 F g^{-1}, respectively).

The lower specific capacitance values recorded for AC-1000 are attributed not only to the smaller surface area of the treated material, but also to the absence of oxygenated functional groups and the pseudocapacitative phenomena associated with them, as demonstrated elsewhere [17]. In terms of cyclability, AC-1000 is more stable

than AC, and what is more important, the loss of capacitance is independent of the operating voltage used, the reduction in the initial specific capacitance values being 4-6 %. The loss of capacitance during cycling is generally believed to be related to irreversible reactions in the capacitor, a parameter which is in turn related to the heteroatom content of the material [27]. The elimination of functionalities during thermal treatment at 1000 ºC yielded an active material with an enhanced cycling stability. Comparable activated carbons reported in the bibliography [12,28] caused, after the same number of cycles, a greater reduction in specific capacitance than that of the present work with AC-1000.

Figure 2.a and 2.b show the effect of long-term cycling on the cyclic voltammograms for sample AC and AC-1000, respectively. In general terms, the voltammograms show the rectangular behaviour typical of SC's which is indicative of a good capacitative performance. These voltammograms also reveal a reduction in specific capacitance values, which is more evident in the case of AC, corroborating the data obtained from the galvanostatic experiments. Additionally, the AC voltammograms show that a significant alteration occurs upon extended cycling, whereas the AC-1000 voltammograms display no such change. For sample AC, the distortion from cycling is more pronounced in the positive-electrode region, particularly when a voltage window of 1 V is used. Moreover, there is a reduction in the anodic current as the window approaches the potential cut-off value, which is more visible at 1 V than at 0.6 V. This indicates the consumption of some of those sites in the active material that are susceptible to irreversible oxidation. At 0.6 V the performance of the cell is closer to that of an ideal SC, as electrostatic charge separation is the predominant mechanism of energy storage. When the operating voltage increases to 1 V, the contribution of pseudocapacitative effects is more pronounced.

Figure 3 shows a representative galvanostatic charge-discharge cycle for AC at 0.6 and 1 V at a constant current load of 500 mA g^{-1}. The triangular shape recorded confirms a good capacitative behaviour and a good charge propagation throughout the active material. A reduction in the time needed for the completion of each cycle after the long-term experiments was also detected, together with a slight increase in the ESR (from ~1.4 to 2 Ω). Closer examination of the cycles reveals that the discharge branches are closer to linearity at 0.6 V than at 1 V, reflecting the greater involvement of faradaic currents when the operating voltage is increased (e.g. electro-oxidation of the surface of the electrode, electrolyte decomposition, etc.), as can be deduced from the voltammograms (Figure 2).

For a detailed study of the changes occurring in the cells, impedance spectroscopy measurements were carried out. A similar trend was observed for both samples, the only remarkable difference being the greater variation in resistance of AC, as can be seen from the ohmic drop represented in the galvanostatic cycles (Figure 3). Figure 4.a shows the Nyquist plot for AC-1000 before and after extensive cycling at 0.6 V, where no significant modifications were recorded. However, when the potential window was increased to 1 V and the long-term experiments were carried out an important change in the shape of the spectrum occurred (Figure 4.b). In the medium-high frequency range there is an increase in the amplitude of the semicircle. This can be attributed to an increase in the intrinsic resistance of the electrode (e.g. incorporation of functional groups due to oxidation, etc.). Despite the stable performance reflected by the specific capacitance values, the shape of the voltammograms and the galvanostatic cycles recorded for AC-1000, extended cycling caused an increase in the resistance of the cell, which is indicative of some form of deterioration. Impedance spectroscopy,

therefore was the only technique that revealed any degradation during the long-term cycling of sample AC-1000.

The results obtained using the two and three-electrode configurations are shown in Figure 5. Figure 5.a contains the charge-discharge cycles obtained for AC at the two operating voltages studied (right Y-axis) and the potential profile where each electrode is operating (left Y-axis). The graph shows that in the completely-discharged state (0 V on the right Y-axis) the anode and cathode are at the same potential (-0.17 V *vs* $Hg|Hg_2SO_4$) defined as *equilibrium potential* or *initial potential* (characteristic of the active material and the media used). When the cell is charged at 0.6 V, the positive electrode reaches +0.12 V *vs* $Hg|Hg_2SO_4$, whereas the negative electrode decreases to -0.47 V *vs* $Hg|Hg_2SO_4$. Thus, each electrode is working at approximately 0.3 V, splitting the total range of potential into equivalent regions. When the cell is charged at 1 V the positive electrode increases its potential to +0.34 V *vs* $Hg|Hg_2SO_4$ and, simultaneously, the negative electrode decreases its potential to -0.67 V *vs* $Hg|Hg_2SO_4$. Once again, the total range of potential is divided into two equivalent ranges of potential. For this sample, the equilibrium potential value remained constant after extended cycling.

A similar trend was obtained for sample AC-1000, the only difference being that the voltage at the initial state is lower than for AC (-0.31 V *vs* $Hg|Hg_2SO_4$). Figure 5.b shows a galvanostatic cycle carried out for sample AC-1000 at 1 V (right Y-axis) and the voltages at which the anode and cathode are operating (left Y-axis). Unlike the case of AC, the initial voltage of the cell increases after extended cycling from -0.31 to -0.06 V vs $Hg|Hg_2SO_4$. However, no clear explanation for this phenomenon has yet been found. The different behaviour of AC and AC-1000 might be related to their dissimilar structural properties, as the carbonized sample has fewer oxygenated functionalities and more unsaturated sites (susceptible to reversible absorption/desorption of hydrogen). It

should also be pointed out that when the cell is in the charged state (1 V, right Y-axis), the negative electrode reduces its potential to -0.82 V *vs* $Hg|Hg_2SO_4$, a potential which is outside the limits of electrochemical stability of the media used (±0.6 V *vs* $Hg|Hg_2SO_4$, as defined by the Nerst equation). Consequently, the negative electrode operates below these limits, producing hydrogen through the pathway: $2H^+(aq.) + 2e^- \rightarrow H_2\ (aq.)\uparrow$. Despite this, the performance of sample AC-1000 is excellent, demonstrating a high overpotential to act as negative electrode.

On the basis of these results an asymmetric device was constructed using AC as the active material of the negative electrode and AC-1000 as the positive one.

3.2.2.- Asymmetric configuration

Figure 6 shows the cyclic voltammograms and galvanostatic cycles obtained for the asymmetric device before and after the long-term experiments. Both representations show the exceptional stability of the capacitor, as the initial behaviour of the cell does not change appreciably. The charge-discharge profiles show a triangular shape with straight charge/discharge branches and the CV curve shows the typical rectangular shape characteristic of EDLC's, indicating a good charge propagation. The specific capacitance values obtained for the first cycle was 220 F g^{-1}, which fell to 210 F g^{-1} after 10,000 galvanostatic cycles, representing a reduction of 4.5 % (and 10 % after 20,000 cycles). Moreover, the asymmetric device leads to an improvement in the energy and power density values of the supercapacitor. After performing 10,000 galvanostatic cycles, the asymmetric device stores 7.0 Wh/Kg, whereas in the case of the using only AC as electrode this values is of 6.90 Wh/Kg and of 6.00 in the case of using AC-1000. Regarding the power density values, the asymmetric system provides 91 W/Kg, whereas

the AC and AC-1000 activated carbons provides 87 and 106 W/Kg, respectively. Consequently, the combination of the two activated carbons in an asymmetric configuration such as that proposed in this work results in a capacitor that combines both the excellent stability of sample AC-1000 (which is less prone to oxidation) and the high capacitance values of sample AC.

4.- CONCLUSIONS

The life cycle of the activated carbons studied was found to be very satisfactory in acidic media, although the thermally treated carbon showed a significantly better behavior.

The initial capacitance of AC-1000 decreased by only ~5 % after 10,000 cycles independently of the operating voltage (0.6 and 1 V), demonstrating that the thermal treatment of AC produces very stable electrode material at both ranges of potential.

The specific capacitance of AC was decreased by 12 % at 0.6 V and 17 % at 1 V after 10,000 cycles due to irreversible reactions associated with the oxygenated functional groups present in this sample, as this introduce instability into the system. Despite this, the capacitance values of AC are still higher than those of AC-1000.

The use of AC as the negative electrode and AC-1000 as the positive one provided an asymmetric capacitor that merges both a high stability and high capacitance values. A decrease of only 10 % in the initial capacitance after 20,000 galvanostatic cycles (4.5 % after 10,000 cycles) was observed.

Acknowledgements.- This work has been carried out with financial support from MEC (project MAT2007-61467) and FICYT (project IB05-086-C1). V. Ruiz acknowledges a predoctoral research grant from FICYT.

REFERENCE

[1] R. Kötz and M. Carlem, Electrochim. Acta, 45 (2000) 2483.

[2] J. L. Figueiredo, M. F. R. Pereira, M. M. A. Freitas, J. J. M. Orfap, Carbon, 37 (1999) 1379

[3] R. C. Bansal, J. B. Donnet, F. Stoeckli, Active Carbon, Marcel Dekker, New York, ch.2, 1988.

[4] E. Frackowiak, F. Béguin, Carbon, 39 (2001) 937.

[5] B. E. Conway, Electrochemical Supercapacitors, Scientific Fundamentals and Technological Applications, Kluwer Academics/Plenum New York, 1999.

[6] A. G. Pandolfo, A. F. Hollenkamp, J. Power Sources, 157 (2006) 11.

[7] K. Jurewicz, K. Babel, A. Źiółkowski, H. Wachowska Electrochim. Acta, 48 (2003) 1491.

[8] M.J. Bleda-Martínez, D. Lozano-Castelló, E. Morallón, D. Cazorla-Amorós, A. Linares-Solano, Carbon 44 (2006) 2642.

[9] C. T. Hsieh, H. Teng, Carbon, 40 (2002) 667.

[10] H. Oda, A. Yamashita, S. Minoura, M. Okamoto, T. Morimoto, J. Power Sources, 158 (2006) 1510.

[11] A. G. Pandolfo and A. F. Hollenkamp, J. Power Sources, 157 (2006) 11.

[12] K. Kierzek, E. Frackowiak, G. Lota, G. Gryglewicz, J. Machnikowski, Electrochim. Acta, 49 (2004) 515.

[13] O. Haas, E.J. Cairns, Ann. Rep. Prog. Chem., Sect. C 95 (1999) 163.

[14] M. F. Rose, C. Johnson, T. Owens, B. Stephens, J. Power Sources 47 (1994) 303.

[15] P. Azaïs, L. Duclaux, P. Florian, D. Massiot, M-A Lillo-Rodenas, A. Linares-Solano, J-P Peres, C. Jehoulet, F. Béguin, J. Power Sources, 171 (2) (2007) 1046.

[16] C. Portet, P. L. Taberna, P. Simon, E. Flahaut, C. Laberty-Robert, Electrochim. Acta, 50 (2005) 4174.

[17] V. Ruiz, C. Blanco, E. Raymundo-Piñero, V. Khomenko, F. Béguin, R. Santamaría Electrochim. Acta, 52 (2007) 4969.

[18] A. Laforgue, P. Simon, J. F. Fauvarque, J. F. Sarrau, P. Lailler, J. Electrochem. Soc. 148 (2001) A1130.

[19] T. Brousse, P. L. Taberna, O. Crosnier, R. Dugas, P. Guillemet, Y. Scudeller, Y. Zhou, F. Favier, D. Be?langer, P. Simon, J. Power Sources 173 (2007) 633.

[20] L. Wang, t. Morishita, M. Toyoda, M. Inagaki, Electochim. Acta 53 (2007) 882.

[21] T. Aida, I. Murayama, K. Yamada, M. Morita, J. Power Sources 166 (2007) 462.

[22] E. Mora, V. Ruiz, R. Santamaría, C. Blanco, M. Granda, R. Menéndez, J.M. Juárez-Galán, F. Rodríguez-Reinoso, J. Power Sources, 156 (2006) 719.

[23] M. M. Dubinin, D. A Cadenhead (Ed.), "Progress in Surface and Membrane Science", Vol. 9, Academic Press, London, 1975.

[24] C. Song, T. Wang, J. Qiu, Y. Cao, T. Cai, J. Porous Materials 15 (1) (2008) 1.

[25] M. Endo, Y. A. Kim, t. Hayahsi, T. Yanagisawa, H. Muramatsu, M. Ezaka, H. Terrones, M. Terrones, M. S. Dresselhaus, Carbon, 41 (10) (2003) 1941.

[26] G. Tremblay, F.J. Vastola, P.L. Walker, Carbon 16 (1978) 35.

[27] B. E. Conway, W. G. Pell, T.-C. Liu, J. Power Sources, 65 (1997) 53.

[28] A. B. Fuertes, G. Lota, T. A. Centeno, E. Frackowiak, Electrochim. Acta 50 (2005) 2799.

FIGURES

Figure 1.- Variation in the specific capacitance values with the number of galvanostatic cycles for samples AC and AC-1000. Influence of the operating voltage. Current load 500 mA g^{-1}.

Figure 2.- Cyclic voltammetry experiments performed for a) AC and b) AC-1000 before and after the long-term cycling. Potential scan rate 1 mV s^{-1}.

Figure 3.- Galvanostatic charge-discharge cycles for AC performed at 0.6 and 1 V before and after the long-term cycling. Current load 500 mA g^{-1}.

Figure 4.- Nyquist plot performed for AC-1000 before and after the long-term cycling at (a) 0.6 V and (b) 1 V.

Figure 5.- a) Galvanostatic cycle for AC at 0.6 and 1 V (solid-line, right-Y axis) and the work potentials for the positive and negative electrodes (dash-line, left-Y axis). b) Galvanostatic cycle for AC-1000 at 1 V (solid-line, right-Y axis) and work potentials for the positive and negative electrodes before and after the long-term cycling (dash-line, left-Y axis). (a.u.= arbitrary units).

Figure 6.- Performance of the asymmetric device before and after the long-term cycling: a) Cyclic voltammetry experiments. Potential scan rate 1 mV s^{-1} and b) galvanostatic charge-discharge cycles at 1 V. Current load 500 mA g^{-1}.

CAPTIONS

Figure 1

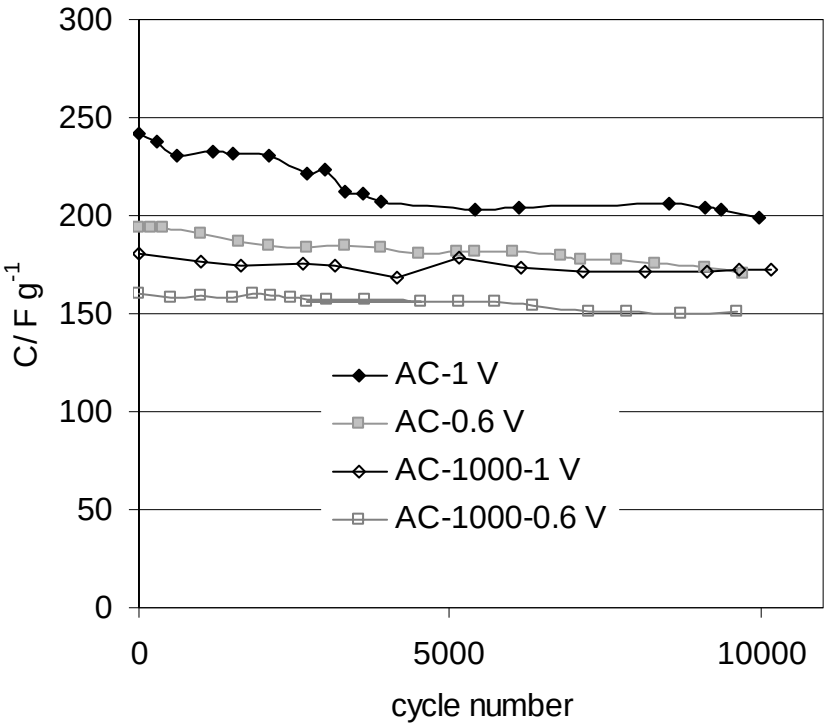

Figure 2

(a)

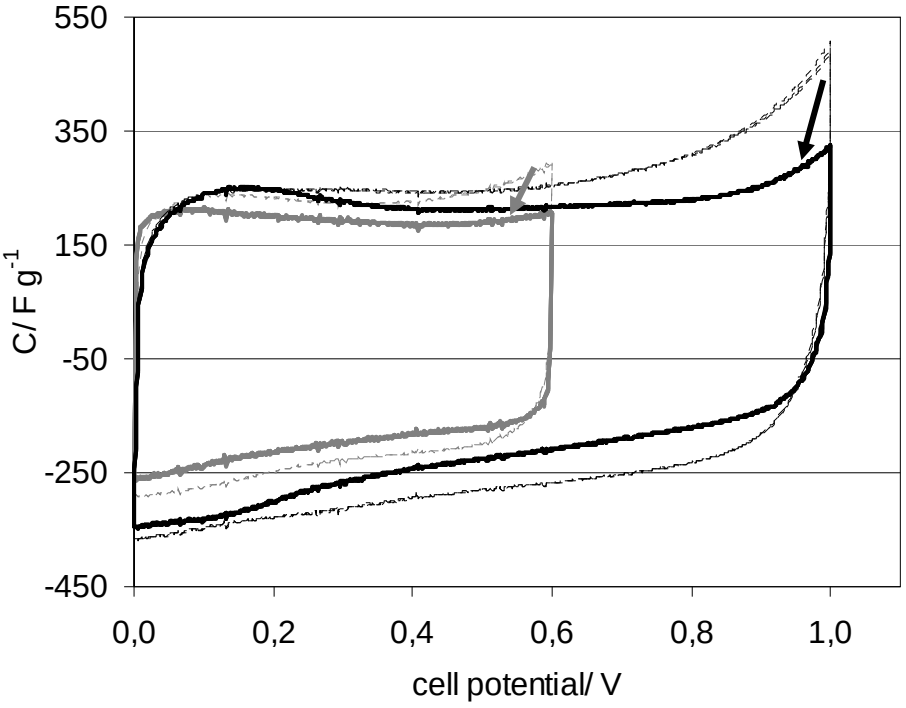
550
350
150
-50
-250
-450
C/ F g-1
0,0
0,2
0,4
0,6
0,8
1,0
cell potential/ V

(b)

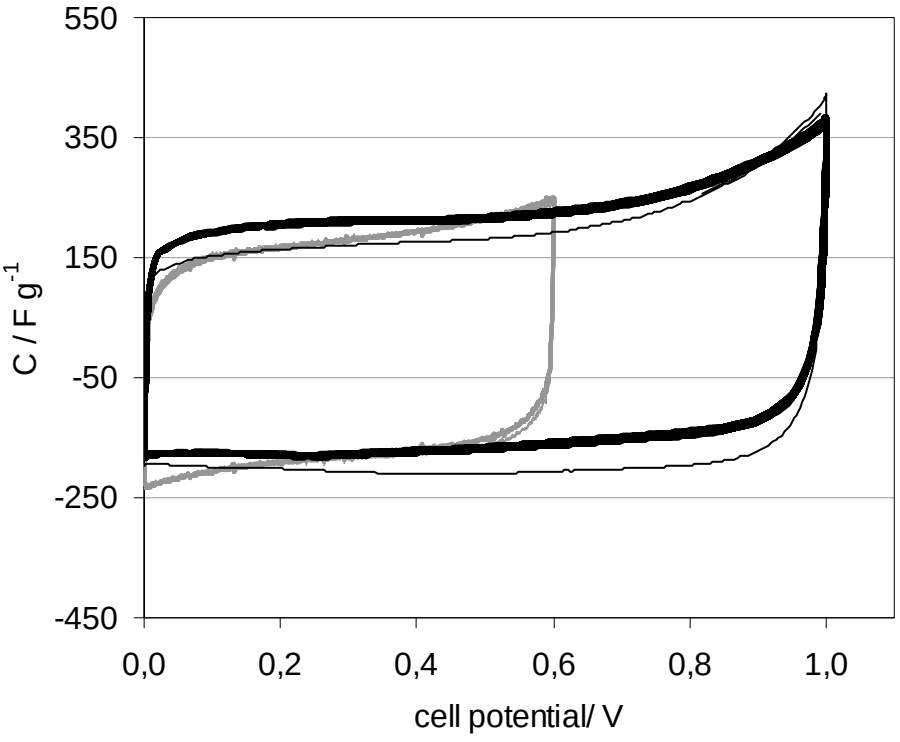
550
350
150
-50
-250
-450
C / F g-1
0,0
0,2
0,4
0,6
0,8
1,0
cell potential/ V

Figure 3

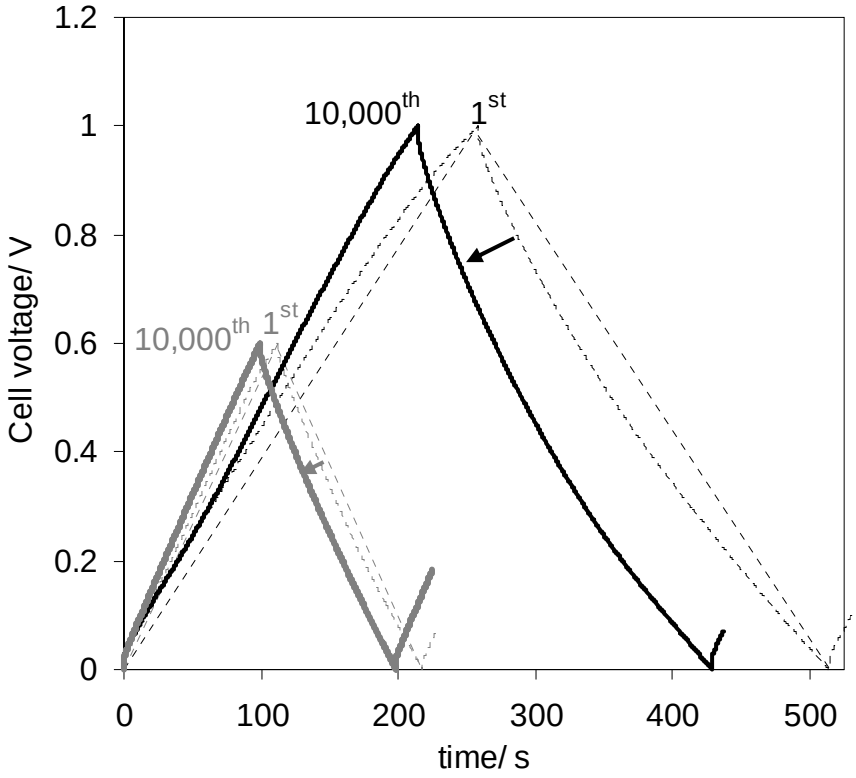
1.2
1
0.8
0.6
0.4
0.2
0
Cell voltage/ V
0
100
200
300
400
500
time/ s
10,000th
1st
10,000th
1st

Figure 4

(a)

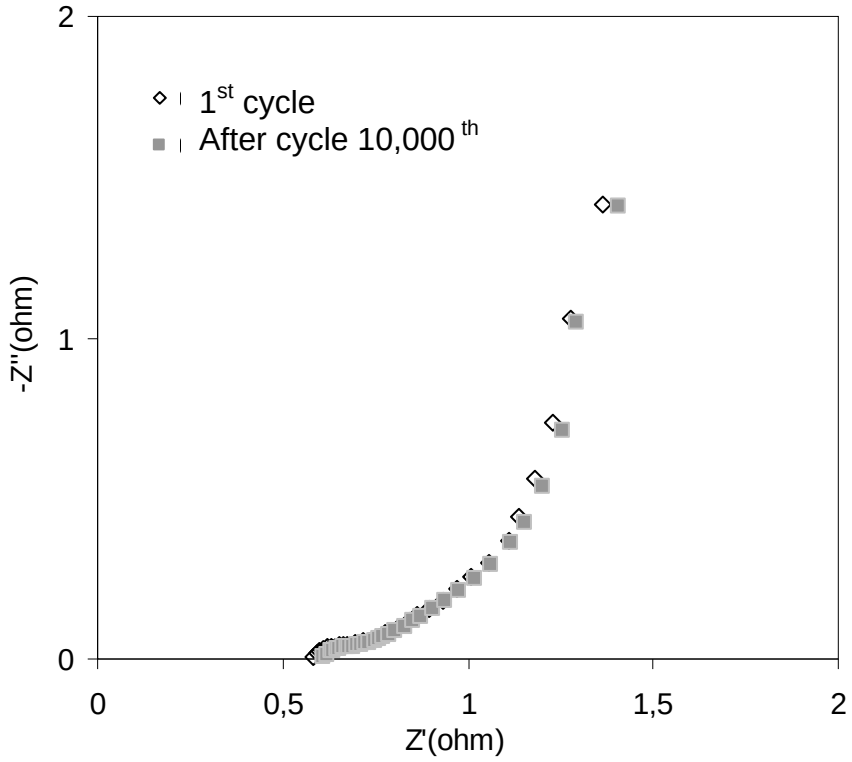
1st cycle
After cycle 10,000 th
-Z''(ohm)
Z'(ohm)
0
0,5
1
1,5
2

(b)

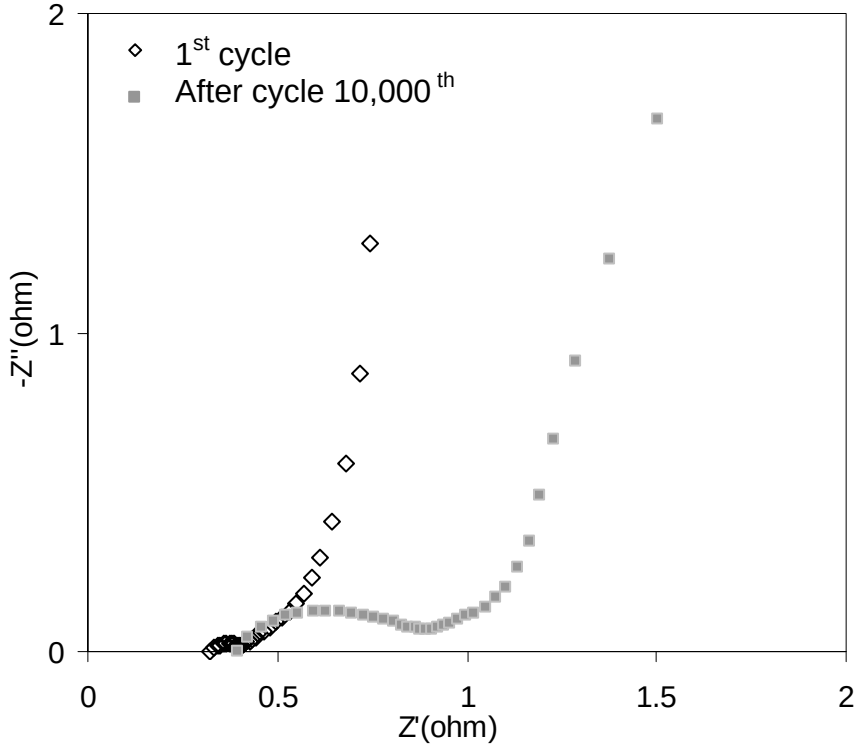
1st cycle
After cycle 10,000 th
-Z''(ohm)
Z'(ohm)
0
0.5
1
1.5
2

Figure 5

a)

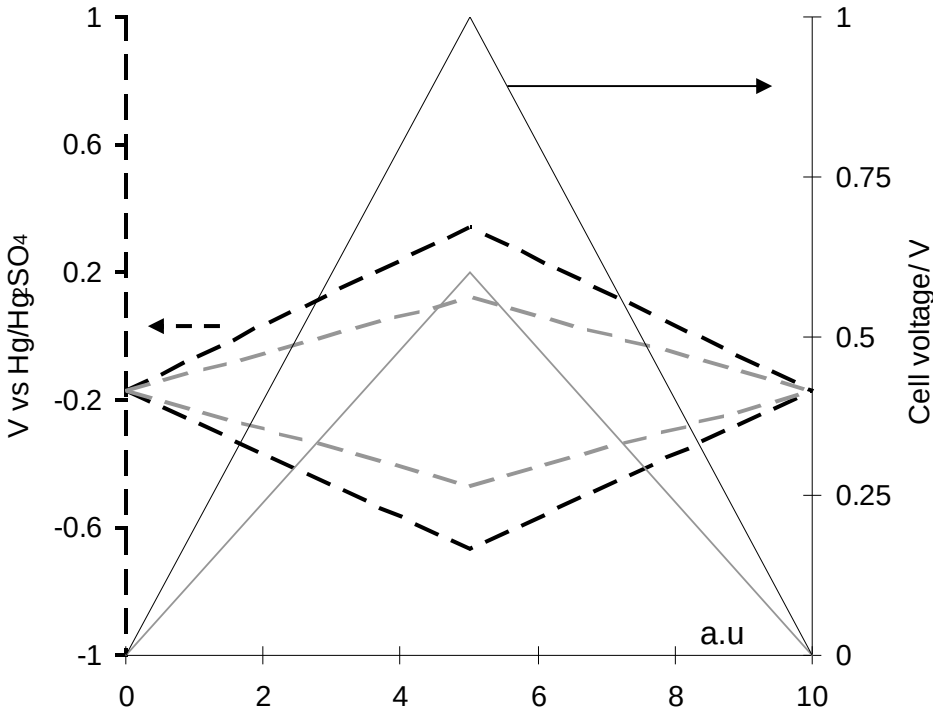
1
0.6
0.2
-0.2
-0.6
-1
V vs Hg/Hg2SO4
0
2
4
6
8
10
a.u
1
0.75
0.5
0.25
0
Cell voltage/ V

b)

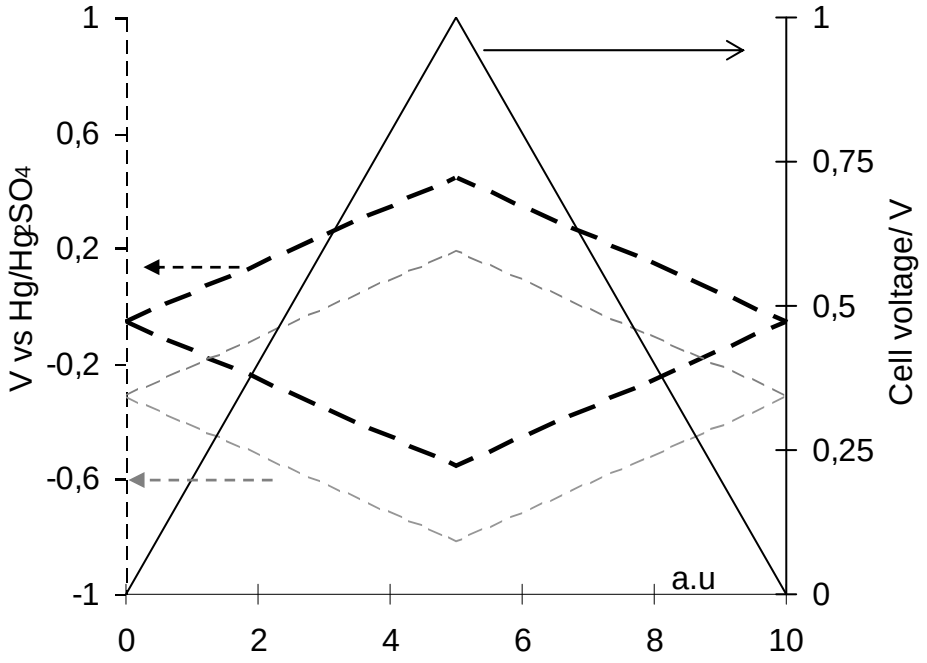
1
0,6
0,2
-0,2
-0,6
-1
V vs Hg/Hg2SO4
0
2
4
6
8
10
a.u
1
0,75
0,5
0,25
0
Cell voltage/ V

Figure 6

a)

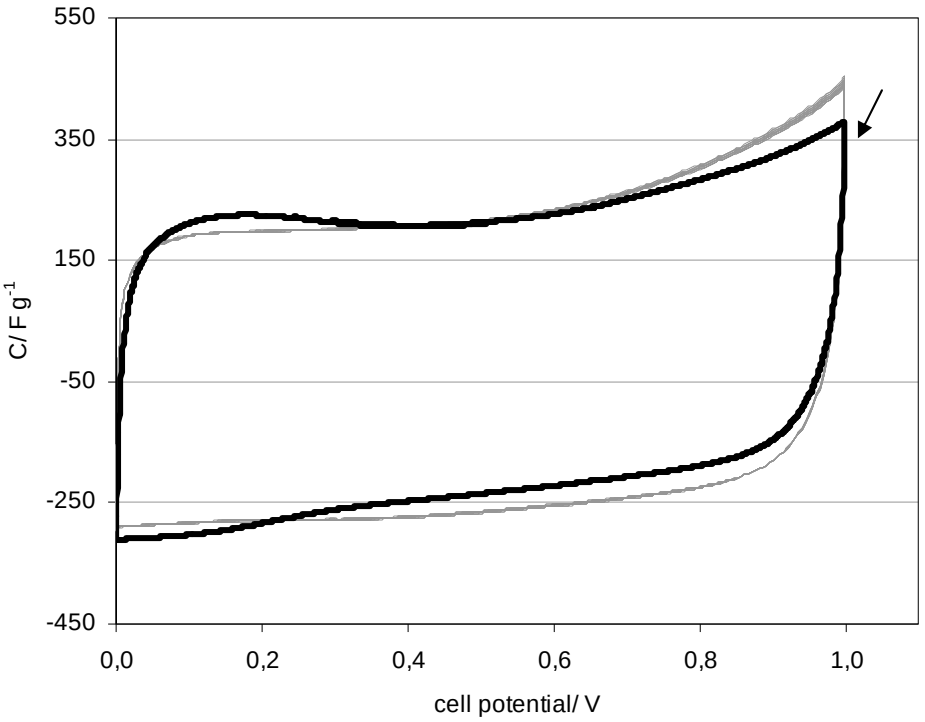
550
350
150
-50
-250
-450
C/ F g-1
0,0
0,2
0,4
0,6
0,8
1,0
cell potential/ V

b)

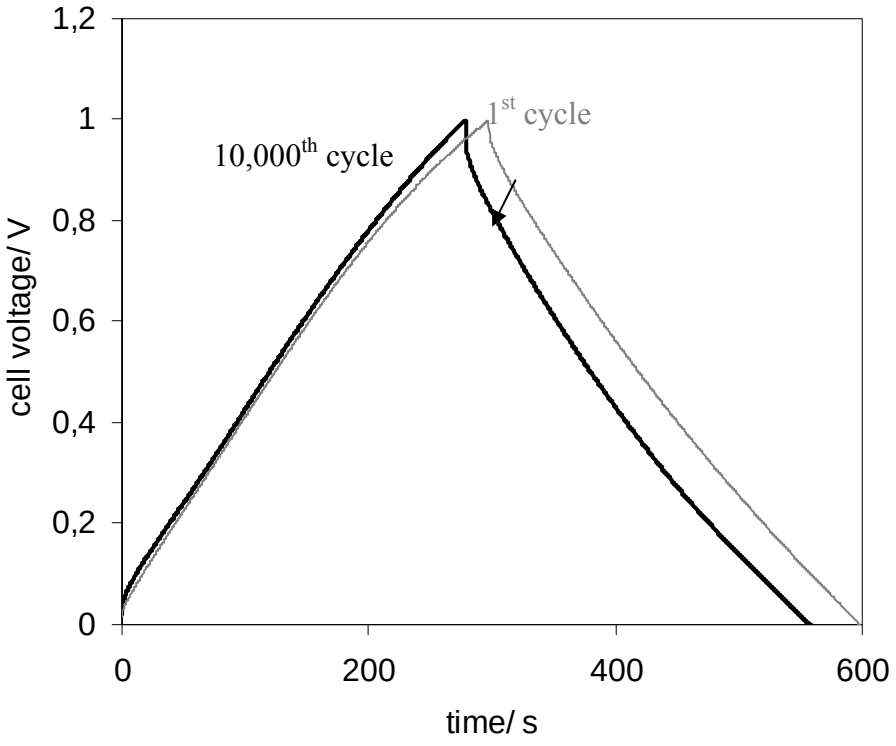
1,2
1
0,8
0,6
0,4
0,2
0
cell voltage/ V
1st cycle
10,000th cycle
0
200
400
600
time/ s